Journal of
Nanomedicine & Nanotechnology

Katsnelson, J Nanomedic Nanotechnol 2012, 3:1
DOI: 10.4172/2157-7439.1000129

Research Article Open Access

Uptake of Some Metallic Nanoparticles by, and their Impact on Pulmonary Macrophages *in Vivo* as Viewed by Optical, Atomic Force, and Transmission Electron Microscopy

B.A.Katsnelson[1]*, L.I.Privalova[1], M.P.Sutunkova[1], M.Ya.Khodos[2], V.Ya.Shur[3], E.V.Shishkina[3], L.G.Tulakina[4], S.V. Pichugova[4] and J.B.Beikin[4]

[1]*Ekaterinburg Medical Research Centre for Prophylaxis and Health Protection in Industrial Workers*
[2]*Ural State University of Economics*
[3]*Ural Federal University*
[4]*Ekaterinburg City Clinical Diagnostics Centre*

Abstract

Optical microscopy (OM), semi-contact atomic force microscopy (sc-AFM), and transmission electron microscopy (TEM) were applied to examine cells in the broncho-alveolar lavage fluid (BALF) obtained from rats 24 hours after instillation of different metallic particles suspended in deionised water or of water without any particles. In a comparative experiment with iron oxide Fe_3O_4 (magnetite) particles having a mean diameter of 10 nm, 50 nm or 1 μm, it was demonstrated that, given equal mass doses, nanoparticles (NPs) induce much more intensive recruitment of phagocytes with a much more significant shift toward neutrophil leukocytes (NL) count in the BALF cell population than micrometric particles do, this shift being an indirect but informative index of particle cytotoxicity for alveolar macrophages (AM). Judging by NL/AM ratio, this cytotoxicity diminishes in the sequence: 10 nm > 50 nm> 1 μm, while judging by OM counts of visible aggregated particles within AMs and NLs and by sc-AFM count of micro-invaginations on the surfaces of these cells, their avidity for particles decreases in the same succession. The same dependence of cell recruitment and of phagocytic activity on NP cytotoxicity was found when the NP diameters were quite similar (ca. 3.5-4.0 nm) but the cytotoxicity of one metal (in our experiment, nanosilver) was higher than that of another (nanogold). TEM pictures of AMs from rats administered the 10 nm magnetite testify to the ability of AMs to actively engulf single NPs and their small aggregates which then form larger conglomerates within fused phagosomes. Some of these large phagosomes lost their membrane, and so freed NPs came into close contact with the nuclear membrane and with mitochondrial membranes and cristae causing their marked damage.

Keywords: Magnetite; Silver and gold nanoparticles; Pulmonary phagocytosis

Introduction

Theoretical grounds for expecting a sharp increase in the toxicity of a substance in the form of nanoparticles (NPs) have been highlighted by many authors (see, e.g., [1-4]. It should be noted, however, that analysis of a great number of published data obtained in actual research supports the statement that "this common perception of greater nanoparticle toxicity is based on a limited number of studies" [5], Moreover, some of the studies do not support this perception (e.g., [6, 7]).

In our own experiments [8-11] with iron oxide Fe_3O_4 (magnetite) particles in nanoscale (10 and 50 nm) and microscale (1 μm) ranges, it was shown that, given equal mass doses, NPs really featured a considerably higher biological aggressiveness than micrometric particles (involving both acute cytotoxicity for pulmonary macrophages when instilled once intratracheally and subchronic toxicity on the organism level when injected repeatedly intraperitoneally). Within the nanometer range, however, the relationship between the diameter and the resorptive toxicity of NPs was found to be intricate and non-unique, which might be attributed to differences in the toxicokinetics controlled by both physiological mechanisms and direct penetration of nanoparticles through biological barriers and by unequal solubility

In industrial conditions, and in environments where ambient air is contaminated with so-called 'ultrafine aerosols', health risks associated with NPs are mainly due to their deposition on free surfaces of the lower airways (or the 'pulmonary region' in aerosol biokinetics terms). The key mechanism underlying the self-clearance of the pulmonary region is the recruitment of cells which are capable of engulfing finest particles, thereby preventing their penetration into the pulmonary interstitium and promoting their elimination by mucociliary transport. The principal effector of this phagocytosis-mediated pulmonary clearance is represented by pulmonary alveolar macrophage (AM), the auxiliary one being neutrophil leukocyte (NL). The recruitment of neutrophils in response to the damaging effect of dust on macrophages plays an important compensatory role. This recruitment is dependent on the amount of macrophage breakdown products, which amount is higher, the higher the damaging effect of particles on the macrophage (particle "cytotoxicity") [12-15]. That is why the ratio of neutrophil to macrophage counts in the cell population of a bronchoalveolar lavage fluid (BALF) can serve an indirect but quite reliable index to the comparative cytotoxicity of different particles [12, 16-18].

It was not clear for some time whether these postulates, well established for particles in the micrometer range, apply to NPs as well. Some researchers maintained that NPs are poorly recognized by

***Corresponding author:** B.A.Katsnelson, Ekaterinburg Medical Research Centre for Prophylaxis and Health Protection in Industrial Workers, Russia, E-mail: bkaznelson@etel.ru

Received December 23, 2011; **Accepted** January 19, 2012; **Published** January 23, 2012

Citation: Katsnelson BA, Privalova LI, Sutunkova MP, Khodos MY, Shur VY, et al. (2012) Uptake of Some Metallic Nanoparticles by, and their Impact on Pulmonary Macrophages *in Vivo* as Viewed by Optical, Atomic Force, and Transmission Electron Microscopy. J Nanomedic Nanotechnol 3:129. doi:10.4172/2157-7439.1000129

protective mechanisms in general and, specifically, that they induce weak attraction of alveolar macrophages, thus being ineffectively eliminated from the lungs [2, 4]. The results of our own experiments, however, contradicted that perception and permitted us to state that the widespread concept of the organism's quasi-defenselessness against NPs should be re-evaluated.

Many of those results have already been published [8-11]. In this paper, we would like to sum up and reconsider them, together with some additional data pertaining to two questions we deem important within the framework of the problem of "pulmonary phagocytic response to nanoparticles". These questions are as follows:

First, while we knew then that the above response depends on NP size for one and the same chemical substance, it seemed logical to expect but still had to be proved that, given the same particle size it should significantly depend on the chemical nature of a substance, specifically, on nano-metal type. To elucidate this point, we decided to compare responses to intratracheally instilled NPs of gold and silver. Because the marked bactericidal activity of nanogold (NG) and nanosilver (NS) renders them usable in partly overlapping fields of practice, comparative assessment of their hazard is not only of theoretical but also of special practical importance. In the literature, there are data obtained on different experimental models suggesting that NG is far less toxic as compared with NS (e.g. [19-26]), but there have been no studies involving a comparative assessment of the phagocytic response to their deposition in lungs.

Second, the data obtained with optical and semi-contact atomic force microscopy should be re-evaluated (and some conclusions based on them re-considered) by comparing them with the results of transmission electronic microscopy (TEM) aimed at visualizing (a) the intracellular distribution of NPs, and (b) their impact on cell ultra-structure. To date, there are not so many published TEM studies carried out by other researchers pursuing the same goals. As a rule, these are *in vitro* studies in which different stable cell line cultures were used.

Thus, Li et al [4] have compared the effect produced on stable cell lines of mice macrophages (RAW 264.7) and human cells of the bronchial epithelium (BEAS-2B) by three fractions of ambient air particles collected in Los Angeles: "coarse" particles with diameters ranging 2.5-10 μm, "fine" plus "ultrafine" particles (<2.5 μm) and "ultrafine" particles (<0.15 μm, i.e. <150 nm[1]). The oxidative stress caused by these particles increased in the order of their listing. TEM showed that although particles of all three types were detectable within macrophages, "coarse" ones were found only in phagolysosomes, while "fine" and, in particular, "ultrafine" particles were found in mitochondria as well, causing marked damage to the latter. It was demonstrated that the uptake of 12.2±1.3 nm gold particles by mouse osteoblastic cells (MC3T3-E1) depended on NP concentration [27]. The authors interpreted their TEM pictures as showing that, when the concentration was high, NP agglomerates were first formed on the outer cell membrane and then were engulfed in the process of endocytosis, while at low concentrations primary single NPs were internalized by diffusion.

Despite doubtless advantages of such *in vitro* experiments (first of all, standardized target cells and controlled exposure conditions), one cannot disregard two obvious disadvantages of them. First, the natural microenvironment in which the particle-cell interaction develops *in vivo* and which cannot be completely imitated *in vitro* may be one of the factors influencing both the kinetics of NP agglomeration outside the cells and the mechanisms of their penetration into cells. Second, although some general mechanisms of this penetration, common to all kinds of cell, may well exist, cells for which the engulfment of live and inanimate particles is one of the most important specific functions may deal with the same NPs in a somewhat different way. Both considerations are of special importance when we discuss the role of the phagocytic response as a mechanism of pulmonary NP clearance. That is why we believe the results of our TEM study performed on macrophages in rat BALF after a single intratracheal instillation of magnetite NPs may be of interest to readers.

[1]"There is no strict dividing line between nanoparticles and non-nanoparticles. The size at which materials display properties different to bulk materials is material-dependent and can certainly be claimed for materials larger in size than 100 nm" [3].

Materials and Methods

We synthesized three samples of chemically identical magnetite (Fe_3O_4) particles of identical magnetisation but of two different nano-sizes (10 and 50 nm) and one micro-size (1 μm, i.e. 1000 nm). In order to obtain NPs with given dimensions we used synthesis in "nano-reactors" / micelles. Strict dosing of iron salts makes it possible to vary NP size and obtain NPs with a sufficiently narrow particle size distribution.

The synthesis was conducted by the following reaction:

$$FeCl_2 + 2FeCl_3 + 8NH_4OH \rightarrow Fe(OH)_2{*}2Fe(OH)_3 + 8NH_4Cl$$

To obtain 10 nm NPs, chloride solutions were mixed, then sodium dioctyl sulfosuccinate (SDS) as a surface-active agent (SAA) as well as n-butanol and n-octane were added in the following ratios:

Composition, %% by weight	Microemulsion 1	Microemulsion 2
aqueous phase, 34	$FeCl_2$ x $4H_2O$ + $FeCl_3$ x $6H_2O$	NH_4OH
organic phase, 44	n-octane	n-octane
SAA, 12	SDS	SDS
Solvent for SAA, 10	n-butanol	n-butanol

The mixture was heated to a temperature of 60°C on a water bath with intensive stirring. Particles were settled by slow, "drop-by-drop" addition of microemulsion 2 to microemulsion 1. The reaction lasted 4 hours at the temperature of 60°C. The particles thus obtained were deposited by centrifugation at 8000 rpm and roasted at a temperature of 600°C. The 50 nm particles were obtained by the same process using cetyl trimethyl ammonium bromide (STAB) as SAA.

The NP size and phase distribution was checked by electronic microscopy [FEI MORGAGNI 286 (D) (US) and Philips CM 300 (Netherland) electronic microscopes]. In both cases the dominant particle size by diameter really falls within the nominal value, i.e. 10 nm or 50 nm, with the particle size distribution in a narrow range around this value. Note, in particular, that in the nominally 10 nm material there were only 8.9 % of 50 nm or larger particles, and in the nominally 50 nm material only 4.4 % of particles under 20 nm in diameter. The magnetic properties of the nanoparticles were confirmed by the Faraday balance method, and the magnetization amounted to 82 emu/g.

Magnetite *microparticles* were obtained by mechanically grinding for 2 minutes the agglomerates obtained by storing 50 nm NPs for 30 days. Then the 1 μm class of particles was separated with the help of a set of sieves. Particle size was checked by optical microscopy. The phase distribution of the microparticles was checked by x-ray phase analysis (a «Dron-2.0" diffractometer, Cu Kα radiation), and the magnetization by the Faraday Balance method.

The method for preparing suspensions (sols) of magnetite particles for toxicological experiments was designed based on the results of research into the kinetics of aggregate formation in micrometric and nanometric particle suspensions in distilled water and in normal saline. This research was carried out by the method of dynamic light scattering on a Brookhaven ZetaPlus universal analyzer of suspensions. It was established that nano-sols of Fe_3O_4 are not stable, and the kinetics of the process of aggregation of a disperse phase depends strongly on the dispersion medium. Water-based sols proved more stable, and for 3-5 min after stopping their exposure on a VCX-750 ultrasonic processor (Sonics and Materials, Inc., US) the nanoparticle aggregation process in them was less dynamic than in sols on the basis of normal saline.

The surface of iron oxide particles was not covered with any polymer or other chemical. Thus. in order to minimise the aggregation inherent in suspensions of many NPs, magnetic ones in particular, we (a) suspended them in de-ionised water and (b) elaborated a technique of intratracheal instillation of ultrasonically dispersed suspensions to rats. The procedure for drawing the suspension into a syringe and its injection into trachea under visual control fell within a time interval (28 s after the ultrasonication, on average) characterised by minimal aggregation of nanoparticles. The aggregation kinetics had been preliminarily studied by the method of dynamic light scattering on a Brookhaven ZetaPlus (USA) universal suspension analyser.

Very stable aqueous suspensions of gold and silver NPs were produced with the help of laser ablation of these metals in water. In the nano-gold (NG) suspension, 99.8% of NPs had a diameter of 3.9±1.8 nm; in the nano-silver (NS) ones, 99.9% and 3.4±1.8 nm, respectively.

All particles compared were administered to outbred laboratory female rats once intratracheally at a dose of 2 mg (for magnetite) or 0.2 mg (for NG and NS)[2] per a rat (of ca. 200 g mass) in 1 ml of sterile deionised water because agglomeration in a suspension in normal saline had been found to occur too quickly. Animals in control groups were administered water without particles by the same routes. Experiments on magnetite particles of different dimensions were run in parallel as well as experiments in which we compared the effects of NG and NS particles.

In a special experiment with magnetite particles, 24 hours after intratracheal instillation of the suspensions under study or of water, the lungs were taken out without bronchoalveolar lavage and homogenized. The decomposition of the homogenized tissue of rats was performed by wet incineration using concentrated sulfuric acid and 30% hydrogen peroxide with heating on Digesdahl Digestion Apparatus Model 23130-20-21 (Hach Company, US) and subsequent evaporation of excessive peroxide and dilution of the solution with tridistilled water. The iron content of the resulting solution was measured by the photometric method described for analysis of waters [28] and adapted by us for the analysis of animal tissues in this study (the adequacy of adaptation was confirmed by the results of analysis of a standard sample of bovine liver). The method allows one to determine 0.05 to 4 mg of iron in 1 dm^3 of solution. The measurements were performed in 5 aliquot samples of the solution from each rat.

As well as performing optical microscopy of sedimented cells following the centrifuging of the bronchoalveolar lavage fluid (BALF), we examined the topography of the BALF cell surfaces under nanometric spatial resolution by the method of semi-contact atomic force microscopy (sc-AFM) with the help of a scanning probe nano-laboratory NTEGRA Therma (Russia) using NSG01 probes with a tip height of 10-15 μm and a tip curvature radius of 10-15 nm.

In a separate experiment, transmission electron microscopy (TEM) was used to study intracellular localisations of magnetite NPs in AMs of the BALF and damage to these cells at ultra structural level that may be attributed to the adverse effect of NPs. Based on the findings of the above studies, we selected AMs exposed to 10 nm NPs for examination under electron microscopy as particles that are more actively phagocytised than the others and, at the same time, are more cytotoxic to AM.

Bronchoalveolar lavage was carried out 24 hours after the instillation of particles. A cannula connected to a Luer's syringe containing 10 ml of normal saline was inserted into the surgically prepared trachea of a rat under hexenal anaesthesia. The fluid entered the lungs slowly under the gravity of the piston, with the animal and syringe positioned vertically.

Particle dia.	Number of cells, mln.			NL/AM ratio
	total	Alveolar macrophages (AM)	Neutrophil leucocytes (NL)	
Control for water	2.53±0.36	2.06±0.29	0.30±0.05	0.15±0.03
10 nm	18.57±3.20*^{Y}	2.72±0.54	14.99±2.57*^{Y}	6.23±0.62*^{Y}
50 nm	26.37±5.12*^{Y}	5.05±0.93*•^{Y}	20.65±4.37*^{Y}	4.42± 0.57*•^{Y}
1 μm	4.06±0.44*•	1.81±0.24	1.93±0,28*•	1.32±0.27*•

«*» – designates values that are statistically significantly different from control value; «•» – same from the value for «10 nm» group; ^{Y} - same from «1 μm» (P<0.05 by Student's t-test)

Table 1: Count of BALF cells 24 hours after intratracheal instillation of suspensions of magnetite particles (2 mg/ml) of various sizes to rats (X±s.e.).

Groups of rats that were administered suspensions of particles with diameters:			
10 nm	50 nm	1 μm	Controls (water)
Iron content (mg/kg raw tissue)			
200 ± 9*	257 ± 8*$^{+}$	258 ± 15*$^{+}$	141 ± 5^{+}
Difference between group administered magnetite and controls			
59 ± 10	116 ± 9^{+}	117 ± 16^{+}	-

*designates values that are statistically significantly different from control value;
$^{+}$ same from the value for the group of rats administered 10-nm particles (P<0.01 by Student's t-test)

Table 2: Iron content of rat lung tissue 24 hours after intratracheal instillation of 2 mg of magnetite particles of various sizes or distilled water (X±s.e.)

[2]Our studies on magnetite particles have been completed when we began to experiment with NG and NS, so first of all we tried to use the same dosage, but a pilot experiment demonstrated that 2.0mg of NS caused too strong an inflammatory response. That is why comparative assessment of responses to NS and NG was carried out at ten times lower doses.

Metal instilled	Number of cells, mln.			NL/AM ratio
	Total	Alveolar macrophages (AM)	Neutrophil leucocytes (NL)	
Control for water	0.99±0.17	0.06±0.01	0.93±0.17	0.05±0.01
Nano-Ag	2.78±0,58*	2.13±0.52*	0.64±0.07	3.17±0.49*
Nano-Au	2.37±0.49*	1.45±0.22*	0.93±0.14	1.67±0.20*•

«*» – designates values that are statistically significantly different from control value; «•» – same from the value for the group of rats administered nano-Ag (P<0.05 by Student's t-test)

Table 3: Count of BALF cells 24 hours after intratracheal instillation of suspensions of gold or silver nanoparticles (0.2 mg/ml) to rats (X±s.e.).

Alveolar macrophages (AM)		Neutrophil leucocytes (NL)	
% AM with 0 – 20 particles	% AM with >20 particles	% NL with 0 – 20 particles	% NL with >20 particles
after administration of 10 nm particles.			
9.38±0.25%^{Y}	90.62±0.35%^{Y}	42.66±0.28%^{Y}	57.34±0.38%^{Y}
after administration of 50 nm particles.			
19.09±0.21%•^{Y}	80.91±0.21%•^{Y}	72.55±0.18%•^{Y}	27.45±0.19%•^{Y}
after administration of 1 μm particles.			
64.00±0.16%•	36.00±0.16%•	97.75±0.08%•	2.25±0.08%•

• designates statistically significant difference from the «10 nm» group; ^{Y} – same from the «1 μm» group (P<0,001 by t-test allowing for standard error of complex means whereby data for each rat are considered as a sample consisting of n cells)

Table 4: Percentage distribution of phagocytising cells with various degrees of particle burden 24 hours after intratracheal instillation of suspensions of magnetite particle (2 mg/ml) of various sizes to rats (X±s.e.).

Then the rat and the syringe were turned 180º, and the fluid flowed back into the syringe. The extracted BALF was poured into siliconized refrigerated tubes. An aliquot sample of the BALF was drawn into a WBC count pipette together with 3% acetic acid and methylene blue. Cell count was performed in a standard hemocytometer (the so-called Goryayev's Chamber). For cytological examination and semi-contact atomic force microscopy (sc-AFM), the BALF was centrifuged for 4 minutes at 1000 rpm, and then the fluid was decanted. For optical microscopy we prepared smears of the sediment on 2 microscope slides. After air drying, the smears were fixed with methyl alcohol and stained with azure eosin. The smears were microscoped with immersion at a magnification of x1000. The differential count for determining the percentage of alveolar macrophages (AM), neutrophil leucocytes (NL) and other cells was conducted up to a total number of 100 counted cells. Allowing for the number of cells in the BALF, these percentages were recalculated in terms of absolute AM and NL counts considered hereinafter (see Results and Discussion).

For the sc-AFM, a 3 μl aliquot of the centrifuged suspension of cells obtained by bronchoalveolar lavage was precipitated on a fresh chip of mica. After 60 seconds, excessive liquid was removed with a paper filter, and the sample was dried up by blowing with clean dry air or nitrogen for 30 sec. It should be noted that the drying of the BALF on a mica surface results in the formation of salt microcrystals, for removing which the sample was washed twice. For washing, the sample was kept for 60 sec on the surface of a drop of deionized water (with the working side down), and then the fluid was removed with the help of a paper filter again. After a repeat washing the sample was dried up finally by blowing with clean dry air or nitrogen for 30 sec.

For performing TEM, BALF was centrifuged for 30 min at 3000 rpm. The cell sediment was fixed in 2.5 % solution of glutaraldehyde with subsequent additional fixing in 1 % solution of osmium tetroxide for 2 hours, then it was washed in 0.2M phosphate buffer and passed through alcohols of increasing concentration and through acetone for dehydration. Then the sample was placed for 24 hours in a mixture of araldite and acetone at a ratio of 1:1, following which it was polymerized in araldite at 37ºC for 1 day and then at 50-60ºC for 2-3 days. Ultra thin sections were obtained on a Leica EM UC6 ultra-microtome, contrasted with lead citrate and examined on a Morgagni 268 electron microscope.

All experiments were carried out on outbred white female rats with the initial body weight of 150 to 220 g. All rats were housed in conventional conditions, breathed unfiltered air, and were fed standard balanced food. The experiments were planned and implemented in accordance with the "International guiding principles for biomedical research involving animals" developed by the Council for International Organizations of Medical Sciences (1985).

Results and Discussion

As can be seen from Table 1, the instillation of iron oxide (magnetite) NPs of both sizes caused a much more intensive increase in the overall cell count of the 24 hours BALF than the instillation of microparticles. However, the response to 10-nm particles was somewhat weaker than that to 50-nm ones. The latter was, probably, due to more effective earlier clearance of the lungs from the finest particles, by virtue of their presumably higher solubility (due to the highest specific surface of the smallest NPs) and, as will be shown below, actually more avid phagocytosis. Indeed, as it is demonstrated by Table 2, the above-the-background (above the control level) iron content 24 hours after an injection of 10 nm magnetite particles was half the content in response to 50 nm and 1 μm particles (in the absence of any difference between the latter two).

Judging by the increase in the NL/AM ratio, the cytotoxicity of 10 nm nanoparticles is a little higher than that of 50 nm NPs, both fractions of the nanometer range being considerably more cytotoxic than the micrometer particles of the same substance (Table 1).

Active recruitment of both types of pulmonary phagocytes, again with a predominance of NLs (and thus with a significant increase in the NL/AM ratio) was demonstrated also 24 hours after intratracheal instillation of gold and silver nano-suspensions (Table 3).

Thus, given comparable NP dimensions, the cytotoxicity of particles and the phagocytic response to their pulmonary deposition depend significantly on the chemical nature of a metal. Specifically, we demonstrated that, judging by the NL/AM ratio, NS is more cytotoxic as compared with NG. It corresponds with the general impression created by a review of the results of many a published study [19-26] according to which the toxicity of NS for different target cells and on

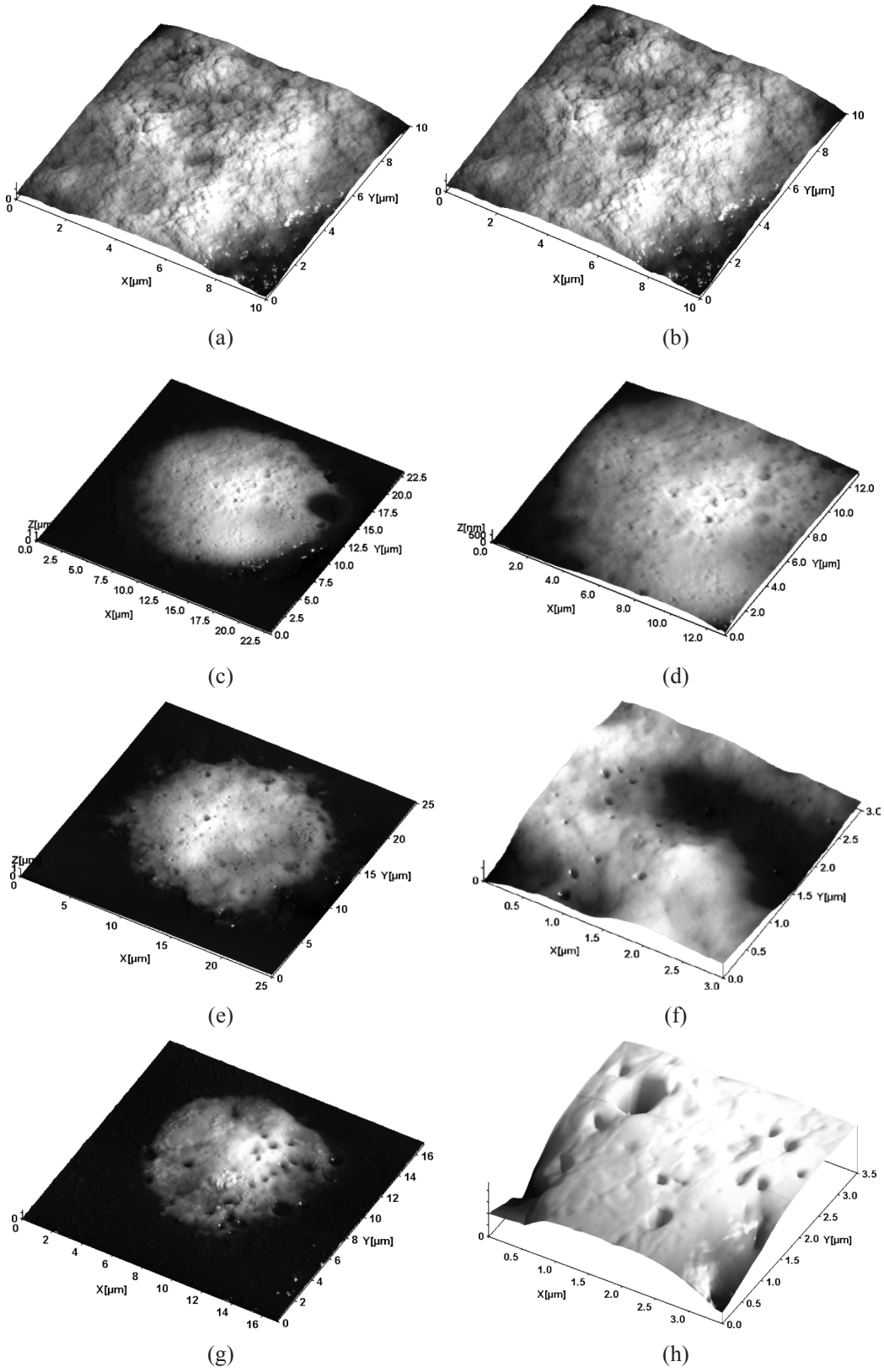

Figure 1: Typical cell surface topography measured by semi-contact AFM, for various groups of samples: (a), (b) controls; (c), (d) after instillation of 10 nm magnetite; (e), (f) 50 nm magnetite; (g), (h) 1 μm magnetite.

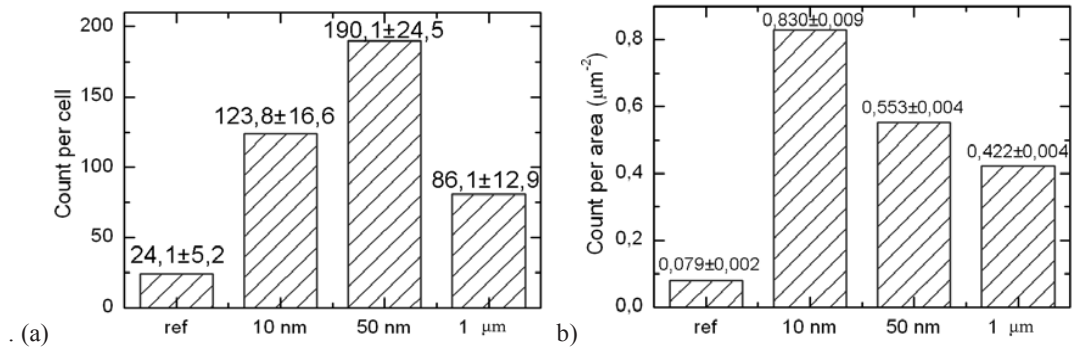

Figure 2: Average number (a) and average surface concentration (b) of micro-pits of all transverse dimensions detected on the surfaces of cells of each group ($x \pm S_x$) (ref – values from the control group).

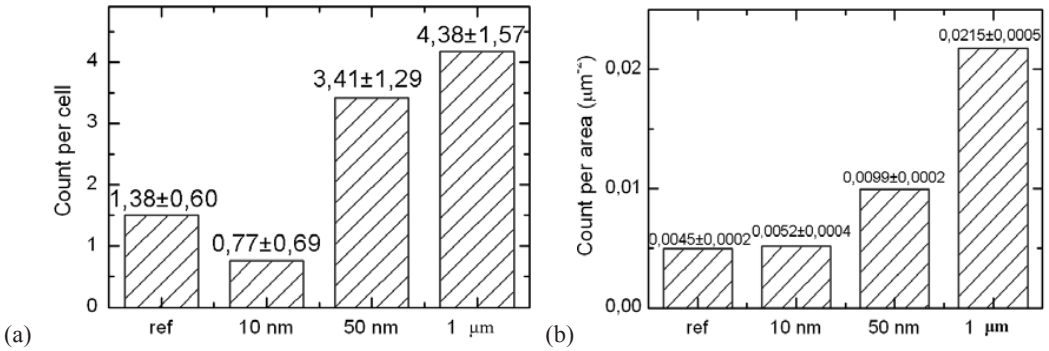

Figure 3: Average number (a) and average concentration (b) of micro-pits with a transverse dimension of >1 μm detected on the surface of cells of each group ($x \pm S_x$). (ref – values from the control group).

the organism level is rather high while that of NG is only moderate to negligible.

We counted particles observable inside the phagocytising cells by means of immersion optical microscopy with a magnification of x1000 (Table 4) in the experiment with iron oxide (magnetite) particles only. It revealed that macrophages and neutrophils loaded with fewer particles constituted a 1.7-2.0 times smaller percentage of the total number of corresponding cells in the BALF from the lungs injected with 10 nm particles in comparison with those administered 50 nm ones, and 2.3-6.8 times smaller as compared with those administered 1 μm ones. On the contrary, the percentage of cells more heavily loaded with visible particles diminished in the sequence: 10 nm – 50 nm – 1 μm.

Thus, the phagocytosis of 50 nm particles was less active while NPs of both sizes were engulfed by both macrophages and neutrophils much more avidly than micrometer ones. The particularly avid phagocytosis of 10 nm particles, along with the presumably higher solubility of the smallest NPs (due to their higher specific surface area), is the probable cause of their less substantial retention in the lungs as mentioned above. It is known that macrophage breakdown products stimulate both the attraction of AMs and, especially, of NLs and the phagocytic activity of macrophages in relation to 1 μm polystyrene test-particles [15]. This suggests an explanation for the direct relationship between the cytotoxicity of magnetite particles of different size and the avidity with which viable phagocytes engulf them.

Micro-pits discovered with the help of sc-AFM on the surface of BALF cells from rats administered iron oxide particles (Figure 1) are interpreted by us as marks left by plasma membrane invagination in the course of particle phagocytosis. The visual assessment of the dependence of the number and comparative diameters of these micro-pits on particle size was confirmed by measurements of the above diameters and by statistical analysis of the results (Figures 2 and 3). Here again we can see that phagocytic avidity (as evidenced by the number of such invaginations per unit area of the cell surface) was maximal in response to 10 nm particles and minimal in response to 1 μm ones. The lower micropits-per-cell count in the case of 10 nm particles as compared with 50 nm (but not with 1 μm!) ones may be explained by a more significant shift in the cell population toward NLs (Table 1), the latter having a smaller surface area than AMs.

On the contrary, the number of large micro-pits (those > 1 μm) per unit area was greatest for 1 μm NPs and lowest for 10 nm ones (Figure 3). It stands to reason that the transverse dimensions of micro-pits (if they are not simply holes in the cell membrane "perforated" by particles but do result from physiological invagination of this membrane) should be much larger compared with particle diameter, although correlating with the latter as it is well seen on the sc-AFM pictures (Figure 1 and 3). When NPs under comparative study have virtually one and the same average diameter, as is the case in our experiment with NPs of silver and gold, micro-pit dimensions prove to be independent of the chemical nature of NPs. Indeed, the average diameter of micro-pits was 87.5±3.5 nm for NG and 80.1±1.8 nm for NS. This difference is not statistically significant, but it is to be reminded that mean NP diameters were much

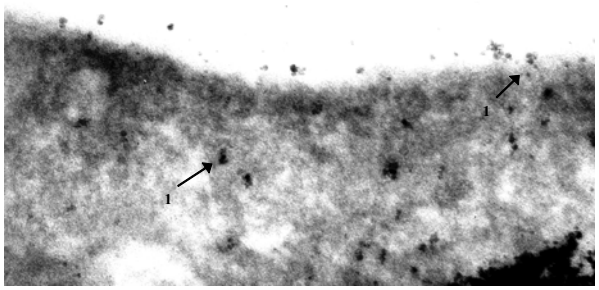

Figure 4: Engulfment of 10 nm magnetite particles by an alveolar macrophage (phagosomes – arrows 1). TEM, magnification *140000.

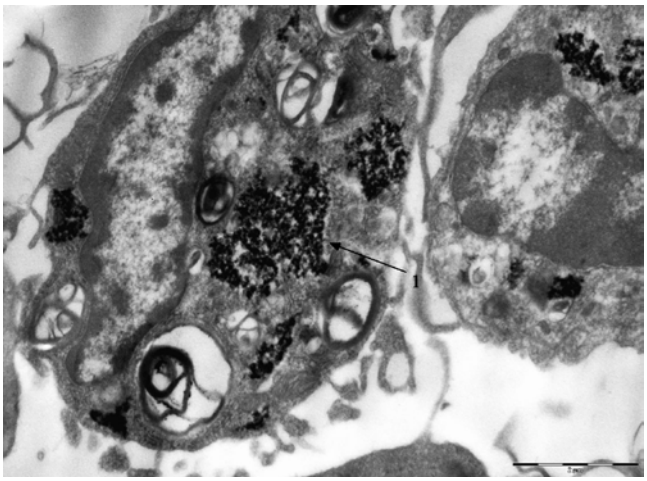

Figure 5: 10 nm magnetite particles in an alveolar macrophage gathered within endosomes (arrow 1). TEM, magnification *8900.

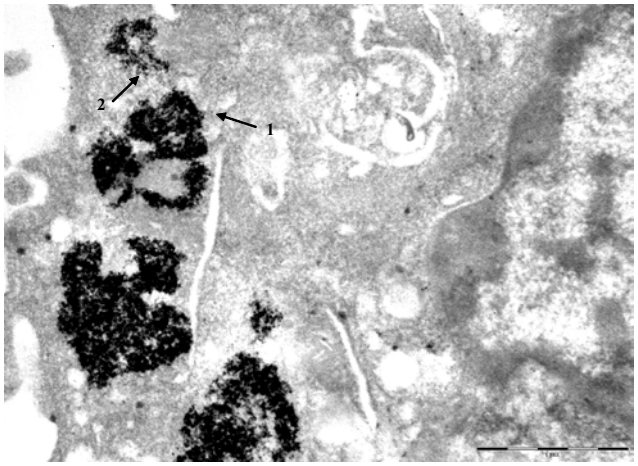

Figure 6: Contact of clustered 10 nm magnetite particles with membranes (arrow 1) and cristae (arrow 2) of an alveolar macrophage's mitochondria. TEM, magnification *22 000.

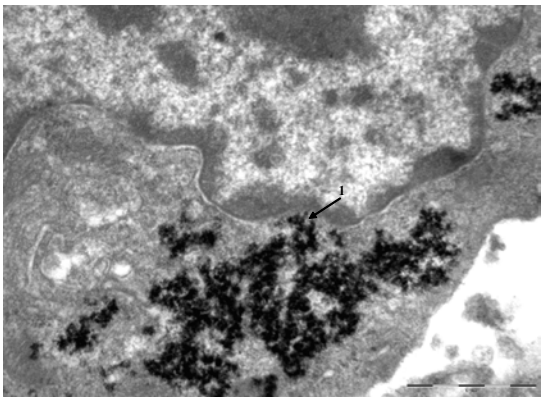

Figure 7: Contact (arrow 1) of clustered 10 nm magnetite particles with the damaged nuclear membrane of an alveolar macrophage. TEM, magnification *22 000.

smaller whilst again being somewhat greater for NG as compared with NS: 3.9 nm and 3.4 nm, respectively. As for the micro-pits count per unit area, it was 1.5 times higher for NS than for NG. Thus we see again that more cytotoxic NPs are being engulfed more avidly.

Figure 4 shows the typical electron microscopy picture of an AM's periphery in rats exposed to magnetite nanoparticles. Extracellular singlet NPs or preformed finest aggregates consisting of 2 or 3 primary NPs are located at a short distance from, or in direct contact with the plasma membrane. Where located within the cell, NPs are frequently found in the vacuoles separated from the cytoplasmic matrix by a membrane. These finest phagosomes are known to form as a result of separation of an invaginated area of the cell's plasma membrane. It can be seen that one such phagosome is in close contact with the internal contour of the plasma membrane, from which, apparently, it has just got separated. Visible closely to it are NPs at the beginning of invagination. It should be qualified, however, that in many cases the boundaries of phagosomes are not clear, and so many NPs visible within a cell could be distributed in cytoplasm in a free state. Whether it is a result of their physical penetration (diffusion) through the cell membrane or that of their secondary liberation after the phagosome's breakdown (see below) is a matter of conjecture and discussion.

None of the sections revealed any pattern that would point to phagocytosis of *preformed* large conglomerates of micrometer size similar to that seen intracellularly under optical microscopy with x1000 magnification. At the same time, electron microscopy also reveals a considerable number of such conglomerates *inside* AM, being separated, in most cases, by a two-contour membrane, i.e. located inside a large endosome (phagosome) presumably resulting from a fusion of finer phagosomes (Figure 5).

In cases where no such separating membrane is visible around an NP conglomerate located in the cytoplasm, we most likely observe a secondary phenomenon associated with a breakdown of the endosomal membrane as a result of the damage caused to it by NPs. This damaging effect is more conspicuous where such free conglomerate of NPs is in contact with the membranes of other organelles (particularly often with those of mitochondria) or with the nucleus membrane as is shown in Figures 6 and 7. Within mitochondria, NPs are found on the membrane and cristae, sometimes filling the matrix up. In these cases, we can observe disturbance of the two-contour appearance of the membranes, breakdown of cristae and clarification of the mitochondrial matrix.

Other researchers [4] have shown that unlike the «coarse fraction» of atmospheric dust, which is detected only within phagosomes in response to *in vitro* exposure of macrophage-like cells, 'ultrafine fraction' particles (up to 150 nm) are observed to be in contact with mitochondria, causing damage to them and related oxidative stress.

Notable in our experiment is the almost total absence of primary lysosomes, which are present in large numbers in the AMs of control animals. This is possibly due to the damaging effect of NPs on the Golgi apparatus responsible for the formation of lysosomes. We cannot rule out, however, that the disappearance of lysosomes can result from the fusion of these organelles with numerous phagosomes (i.e. the formation of phagolysosomes, or the so-called secondary lysosomes). Following the disruption of phagolysosomal membranes, the liberation of lysosomal hydrolases in the cytoplasm is likely to be an important additional mechanism of cell damage and destruction. Indeed, under electron microscopy we found quite a few completely destroyed AMs with NPs and their conglomerates escaping into the intercellular space. The role of such "self-digestion" of macrophages at exposure to silica microparticles was postulated a long time ago [29] and has found its way into the circle of classical ideas concerning the pathogenesis of silicosis [18].

Thus, the results of the TEM examination confirm that the AM is quite capable of recognizing and phagocytising even the finest particles of the nanometric range. Here we do not deal with the mechanical penetration or, in any case, with just the mechanical penetration of such NPs through the plasma membrane but also with an active physiological process following the general pattern of phagocytosis of any solid particles. Moreover, there are sufficient grounds to believe that the formation of intracellular conglomerates of NPs is essentially linked not simply to their special predilection to physical aggregation characteristic of all NPs (magnetic ones especially) in liquid medium, but first of all to the same physiological process at the stage during which fine phagosomes fuse into larger ones inside which this predilection ultimately manifests itself. Finally, the findings provide evidence in favour of the hypothesis that, as well as in response to the effect of mineral microparticles, the primary cause of NP cytotoxicity for AM is their membranolytic activity.

Conclusion

We believe that, taken as a whole, the experimental data summarized and discussed in this paper demonstrate that:

(a) *In vivo* uptake of metallic nanoparticles by specialized phagocytizing cells functioning on the free surface of the pulmonary region is due to a physiological process (endocytosis) rather than to penetration (diffusion) under physical forces.

(b) This process is supported by a defensive reaction consisting in the recruitment of large numbers of AMs and NLs onto the above free surface, the NL/AM ratio being higher, the smaller the NP size or the more toxic the nano-metal.

(c) Internalized NPs can markedly damage (up to death and destruction) the phagocytizing cell, presumably, through their membranolytic action.

In total, our data agree with the prevailing perception of the intrinsically high bio-aggressiveness of nanomaterials but make us believe that the no less widespread concept of the organism's quasi-defenselessness against NPs should be critically re-evaluated.

References

1. Donaldson K, Stone V, Tran CL, Kreyling W, Borm PJ, et al. (2004) Nanotoxicology. Occup Environ 61: 727-728.
2. Oberdörster G, Oberdörster E, Oberdörster J (2005) Nanotoxicology: An Emerging Discipline Evolving from Studies of Ultrafine Particles. Envitonm Health Perspect 113: 823-839.
3. Neus G.Bastus, Eudald Casals, Socorro Vazquez-Compos, Victor Puntes (2008) Reactivity of Engineered Inorganic Nanoparticles and Carbon Nanostructures in Biological Media. Nanotoxicology 2: 99-112.
4. Li N, Xia T, Nel Ae (2008) The Role of Oxidative Stress in Ambient Particulate Matter-Induced Lung Diseases and Its Implications in the Toxicity of Engineered Nanoparticles. Free Radic Bio Med 44: 1689-1699.
5. David B. Warheit, Kenneth L. Reed, Chritie M. Sayes (2009) A role of surface reactivity in TiO_2 and quartz-related nanoparticle pulmonary toxicity. Nanotoxicology 3: 181-187.
6. Warheit DB, Webb TR, Colvin Vl, Reed kl, Sayes CM, et al. (2007) Pulmonary bioassay studies with nanoscale and fine-quartz particles in rats: toxicity is not dependent upon particle size but on surface characteristics. Toxicol Sci 95: 270-280.
7. Klarisson Hl, Gustaffson J, Cronholm P, Möller L (2009) Size-dependent toxicity of metal oxide particles – a comparison between nano- and micrometer size. Toxicol Lett 188: 112-118.
8. Katsnelson B, Privalova Li, Kuzmin Sv, Degtyareva TD, Sutunkova MP, et al. (2010) Some peculiarities of pulmonary clearance mechanisms in rats after intratracheal instillation of magnetite (Fe_3O_4) suspensions with different particle sizes in the nanometer and micrometer ranges: are we defenseless against nanoparticles? Int J Occupat and Environ Health 16: 508-524.
9. Katsnelson BA, Privalova LI, Degtyareva T, Sutunkova (2010) Experimental estimates of the toxicity of iron oxide Fe_3O_4 (magnetite) nanoparticles. Central Eur J Occup and Envir Medic 16: 47-63.
10. Katsnelson BA, Degtyareva TD, Minigalieva II, Privalova LI, Kuzmin Sv, et al. (2010) Sub-chronic systemic toxicity and bio-accumulation of Fe_3O_4 nano- and microparticles following repeated intraperitoneal administration to rats. Internat J Toxicol 30: 59-68.
11. Katsnelson Ba, Privalova Li, Sutunkova Mp, Tulakina Lg, et al. (2011) The "*In Vivo*" Interaction Between Iron Oxide Fe_3O_4 Nanoparticles And Alveolar Macrophages. Bull Exptl Biol Medic 151, 11: 560-565.
12. Katsnelson BA, Privalova LI (1984) Recruitment of Phagocytizing Cells into the Respiratory Tract as a Response to the Cytotoxic Action of Deposited Particles. Environ Health Perspect 55: 313-325.
13. Privalova LI, katsnelson BA, yelnichnykh LN (1987) some peculiarities of the pulmonary phagocytotic response, dust kinetics, and silicosis development during long term exposure of rats to high quartz levels. Brit j ind med 44: 228-235.
14. Privalova LI, katsnelson BA, Osipenko AB, Yushkov BN, Babushkina LG, et al. (1980) Response of a phagocyte cell system to products of macrophage breakdown as a probable mechanism of alveolar phagocytosis adaptation to deposition of particles of different cytotoxicity. Environm health perspect 35: 205-218.
15. Privalova LI, Katsnelson BA, Sharapova NY, Kislitsina NS (1995) On the relationship between activation and the breakdown of macrophages in pathogenesis of silicosis Medic lavoro 86: 511-521.
16. Katsnelson BA, Konyscheva LK, Sharapova NYE, Privalova LI (1994) Prediction of the comparative intensity of pneumoconiotic changes caused by chronic inhalation exposure to dusts of different cytotoxicity by means of a mathematical model. Occup environ med 51: 173-180.
17. Katsnelson BA, Konysheva Lk, Privalova LI, Sharapova NY (1997) Quartz dust retention in rat lungs under chronic exposure simulated by a multicompartmental model: further evidence of the key role of the cytotoxicity of quartz particles. Inhalation Toxicology 9: 703-715.
18. Katsnelson BA, Alekseyeva OG, Privalova LI, Polzik EV (1995) Pneumoconioses: The Pathogenesis And Biological Prophylaxis. Ekaterinburg: The Urals Division of the Ras 325.
19. Ahamed M, Alsalhi MS, Siddiqui MK (2010) Silver Nanoparticles Applications and human health. Clinica chimica acta 411 (23-24): 1841-1848.

20. Ahmadi F, Kordestany AH (2011) Investigation On Silver Retention In Different Organs And Oxidative Stress Enzymes In Male Broiler Fed Diet Supplemented With Powder Of Nano Silver. Amer-Eurasian J Toxicol Sci 3: 28-35.

21. Asharani Pv, Lianwu Y, Gong Zh, Valiyaveettil S (2010) Comparison Of The Toxicity Of Silver, Gold And Platinum Nanoparticles In Developing Zebra Fish Embryos. Nanotoxicology 5: 43-54.

22. Bakri SJ, Pulido JS, Mukerjee P, Marler RJ, Mukhopadhyay D, et al. (2008) Absence of histologic retinal toxicity of intravitreal nanogold in a rabbit model. Retina 28: 147-149.

23. Balasurbamanian Sk, Jittiwat J, Manikandan J, Ong CN, Yu LE, et al. (2010) Biodistribution of gold nanoparticles and gene expression changes in the liver and spleen after intravenous administration in rats. Biomater 31: 2034-2042.

24. Chen YS, Hung YC, Liau I, Huang GS (2009) Assessment Of The *In Vivo* Toxicity Of Gold Nanoparticles. Nanoscale Res Lett 8: 858-864.

25. Glazer ES, Zhu C, Hamir An, Borne A, Thompson CS, Curley SA, et al. (2010) Biodistribution And Acute Toxicity Of Naked Gold Nanoparticles In A Rabbit Hepatic Tumor Model. Nanotoxicology 5: 459-468.

26. Park EJ, Bae E, Yi J, Kim Y, Choi K, et al. (2010) Repeated-dose toxicity and inflammatory responses in mice by oral administration of silver nano-particles. Environ toxicol pharmacol 30: 162-168.

27. Mustafa T, Watanabe F, Monroe W (2011) Impact Of Gold Nanoparticle Concentration On Their Cellular Uptake By Mc3t3-E1 Mouse Osteoblastic Cells As Analyzed By Transmission Electron Microscopy. J Nanomedic Nanotechnol 2: 118

28. Lurje Yy (1973) Standardized methods for analyzing waters. Moscow: Publishing House “Khimiya” (Russian).

29. Allison A.C. (1971) Lysosomes And The Toxicity Of Particulate Pollutants. Arch Intern Med 128: 131-139.